

# 🍋 → 🍷: Squeeze Out Tokens from Sample for Finer-Grained Data Governance

Weixiong Lin<sup>1,2</sup>, Chen Ju<sup>1✉</sup>, Haicheng Wang<sup>1,2</sup>, Shengchao Hu<sup>2</sup>, Shuai Xiao<sup>1✉</sup>,  
Mengting Chen<sup>1</sup>, Yuheng Jiao<sup>1</sup>, Mingshuai Yao<sup>1</sup>, Jinsong Lan<sup>1</sup>, Qingwen Liu<sup>1</sup>, Ying Chen<sup>1</sup>  
<sup>1</sup> Alibaba Group    <sup>2</sup> Shanghai Jiao Tong University

wx\_lin@sjtu.edu.cn, cju.void@gmail.com, {shuai.xsh, yingchen}@gmail.com

## Abstract

Widely observed data scaling laws, in which error falls off as a power of the training size, demonstrate the diminishing returns of unselective data expansion. Hence, data governance is proposed to downsize datasets through pruning non-informative samples. Yet, isolating the impact of a specific sample on overall model performance is challenging, due to the vast computation required for tryout all sample combinations. Current data governors circumvent this complexity by estimating sample contributions through heuristic-derived scalar scores, thereby discarding low-value ones. Despite thorough sample sieving, retained samples contain substantial undesired tokens intrinsically, underscoring the potential for further compression and purification. In this work, we upgrade data governance from a ‘sieving’ approach to a ‘juicing’ one. Instead of scanning for least-flawed samples, our dual-branch DataJuicer applies finer-grained intra-sample governance. It squeezes out informative tokens and boosts image-text alignments. Specifically, the vision branch retains salient image patches and extracts relevant object classes, while the text branch incorporates these classes to enhance captions. Consequently, DataJuicer yields more refined datasets through finer-grained governance. Extensive experiments across datasets demonstrate that DataJuicer significantly outperforms existing DataSieve in image-text retrieval, classification, and dense visual reasoning.

## 1. Introduction

Vision-language pretraining (VLP) [26, 42, 74, 86] is the cornerstone of foundation models (FM) [2, 43, 59] during their pursuing for artificial general intelligence (AGI) [3, 21]. CLIP [62] as an example of vision-language models (VLMs), used as default initialization in AIGC models [25, 69], multi-modal large language models (MLLMs) [10, 87], etc. Despite the essential role that large-scale web data now play in VLP, unselective data expansion hits diminishing returns due to the power-law nature of scaling laws [67]. Excess samples contribute minimal novel information while

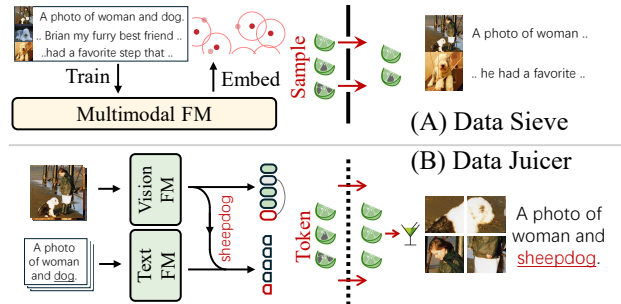


Figure 1. (A) **Data Sieve** relies on multi-modal foundation models (FMs) to retain high-value samples. The hurdle of sample value estimation necessitates the use of manually-designed strategies for governance, limiting Data Sieve’s generalizability across datasets. (B) **Data Juicer** employs the vision FMs to retain informative image patches, and the text FMs to enhance captions by incorporating visual semantics. The automatic pipeline yields more accurate and generalizable sample refinement through finer-grained governance.

potentially introducing noise, leading to poor performance on various downstream tasks.

To address this challenge, data governance is proposed to elitize the dataset by selecting only informative samples for training, thereby optimizing model performance (Tab. 1). Coreset selection, for instance, develops score functions and discards superfluous data points, though these have largely been at sub-ImageNet scale [61, 71]. Data pruning aims at large-scale data governance and develops self-supervised pruning metrics, yet primarily evaluated on vision-only models [67]. **DataSieve** extends similar idea to multi-modal data, prioritize image-text pairs selection according to samples’ contributions [1, 67, 70, 73].

Yet, isolating the impact of samples on overall model performance is challenging. Current DataSieves circumvent this complexity by using heuristic-based metrics as an approximation (e.g. the distance to near centroid, similarity with neighbors) [70]. Despite sample-wise sieving for de-duplication and diversification, the substantial undesired image pixels and caption words within retained samples are unaddressed [73]. Also, image-text alignment is crucial

Method	Data Type	Supervision	Granularity	Estimation	Alignment	Large-scale	Year
Coreset Selection [61]	Image	Class Label	Sample	heuristic	-	✗	2021
Data Pruning [67]	Image	Self Supervision	Sample	heuristic	-	✓	2022
DataSieve [1, 70, 73]	Multi-modality	Image-text Pairs	Sample	heuristic	✗	✓	2024
DataJuicer (Ours)	Multi-modality	Image-text Pairs	Patch / Token	model-derived	✓	✓	-

Table 1. **Data Governance Methods.** Our DataJuicer differs from DataSieve in granularity. It extends data governance to image-patch/word-token level. With model-derived contribution estimation, DataJuicer can smoothly scale to large data spared from heuristic-induced biases. We further improve image-text alignment by enhancing captions with visual evidence.

to VLP, while DataSieve is merely choosing the best from inherently misaligned web data. Such coarse-grained data governors manage to eliminate easily identified low-quality samples, but their heuristic nature also leads to biases. While beneficial at smaller scales, the gains of DataSieve erode with increasing data scale and may even turn detrimental [22].

Motivated by these observed limitations of DataSieve, we take one step back and ask, is it possible to combat these limitations with finer-grained data governance?

Our exploration upgrades data governance from a sieving approach to a ‘juicing’ one (Fig. 1). Instead of scanning for least-flawed samples, our DataJuicer cracks each sample (image, caption) into token-level ingredients (patches, words). We employ dual-branch to squeeze out informative tokens only. (1) *Vision Branch* uses Vision FMs (e.g. DINO [4]) to patchify the image and perform token-wise reduction. Most contributive patches are retained based on model-derived estimation from Vision FMs’ attention mechanism. Vision FMs also identify relevant object classes present in the image. (2) *Text Branch* use Language FMs (e.g. LLaMA) to correct text imperfections such as misspellings and repetitive expressions. Also, the visual evidences from the vision branch are incorporated, we use high-confidence object classes to rectify captions for better-aligned image-text pairs. Note that DataSieve and DataJuicer are complementary rather than mutually exclusive, and their combined use can further enhance data governance.

We show through comprehensive experiments that DataJuicer significantly enhances data efficiency during training and improves performance on over ten downstream tasks. Furthermore, our findings indicate that DataJuicer performs effectively without incurring computational overhead. Thorough ablations are done to reveal each component’s effectiveness, both quantitatively and qualitatively.

To sum up, our contribution lies in three folds:

1. We propose juicing-based data governors different from sieving-based ones, providing a finer-grained pipeline to produce high-quality image-text pairs.
2. We design DataJuicer to reduce undesired tokens and enhance cross-modal alignment, by using vision/language FMs for automatic model-derived token-value estimation.
3. We conduct extensive experiments and ablations on many benchmark datasets, demonstrating the data improvements achieved by our DataJuicer and showcasing the superior performance of trained VLMs.

## 2. Related Works

**Foundation Models (FMs)** trained on large-scale datasets have significantly advanced progress in both CV and NLP. FMs are generally classified into two categories: uni-modal FMs and multi-modal FMs. (1) Uni-modal FMs capture deep, domain-specific knowledge by training on large-scale intra-modal data, such as DINO [4] and LLaMA [72]. (2) Multi-modal FMs have seen rapid advancements, with notable models including GPT-4V [59] and LLaVA [43]. Uni-modal FMs play a crucial role in multi-modal FMs by providing specialized, in-depth knowledge within their domains.

**Vision-Language Pretraining (VLP)** establish cross-modal alignment by leveraging large-scale web-sourced datasets, as exemplified by models such as CLIP [62], ALIGN [26], Florence [83], FILIP [79], and PMC-CLIP [42]. VLP architectures are grouped into three types: single tower [9, 36], twin towers [26, 62], and bridge tower [39, 40, 90]. In terms of optimization techniques, contrastive learning [7, 89] and cross-modal matching [11, 39] dominate, with applications ranging from self supervision [44, 47], weak supervision [14, 15, 40], to partial supervision [33, 46]. As a foundation for multi-modal FMs, VLPs contribute to various downstream tasks, including image perception [8, 13, 19, 32, 35, 57], video understanding [12, 27, 28, 30, 34, 45, 46, 75, 88], open-vocabulary learning [29, 31, 53, 54, 77, 78] and AIGC generation [6, 52, 55, 76]. Notably, most multi-modal FMs initialize their visual encoders using pre-training like CLIP.

**Data Governance.** Large-scale image-text data are crucial for building powerful VLMs, which serve as the foundation for multi-modal FMs. While VLPs consume data at a rapid rate, far exceeding the volume that can be manually curated, necessitating the use of automated data pipelines for web-collected data [63]. However, web-sourced data often suffer from noise and redundancy, leading to suboptimal VLP performance. As in Tab. 1, recent data governance explores to address these challenges [1, 70, 73]. These approaches break through the vision-only constraints of Coreset Selection and Data Pruning by sieving out contributive image-text pairs with heuristic-estimated informativity, a framework we term DataSieve. De-duplication and diversification are two main goals of DataSieve. It employs the visual embeddings of samples for clustering and discards those proximal to centroids to reduce semantic overlapping samples similarity [1]. Dedicate sampling strategies are also

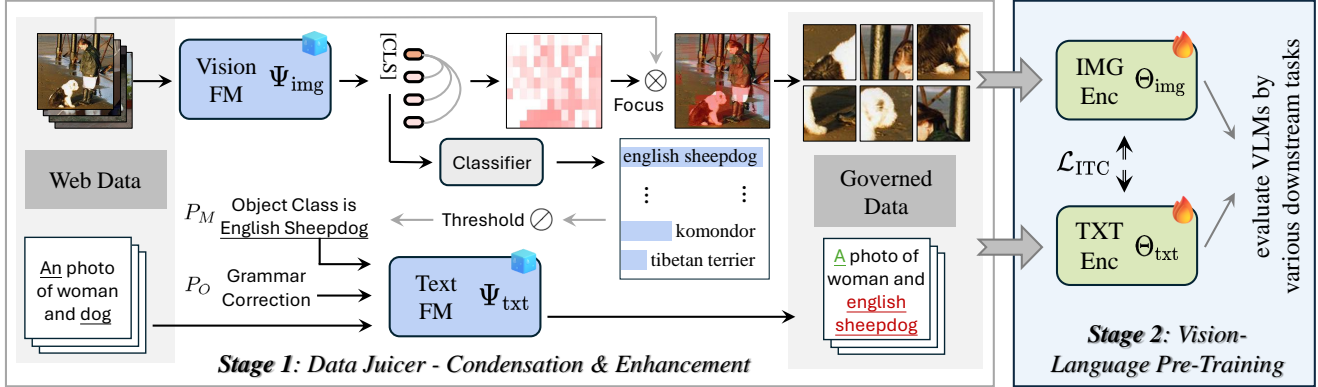


Figure 2. **Pipeline Overview.** Our framework employs vision and text branches to reduce undesired ingredients in real-world data. Vision Foundation Model (FM) is used to discard image patches with low contribution to overall semantics and to extract object classes. Text Foundation Model (FM) rectify grammatical errors and refine the textual descriptions. By incorporating high-confidence class names, the text branch enhances image-text consistency. This process results in data that is both less redundant and less noisy, therefore leading to more effective training of Vision-Language Pretraining.

developed to mine neighboring relationships among samples, thereby enhancing data diversity [56]. DataSieves focus on scanning least-flawed samples while ignoring the image-text misalignment. Some attempts to synthesize captions with MLLM [18, 37, 73, 85], though effective, the generated captions tend to be homogenized, reducing the diversity and richness of the provided information when more samples are modified. The use of MLLMs for captioning actually introduces a paradox of mutual dependence between VLMs and MLLMs: Advancements in VLMs are prerequisites to enhancing the recaptioning capabilities of MLLMs. Furthermore, these models tend to prioritize text, often overlooking redundancy within image pixels.

### 3. Methods

#### 3.1. Notations and Preliminaries

**Task Formulation.** Given training budgets  $\mathcal{T}$ , data governor  $\Psi$  is to construct a governed dataset  $\mathbb{V}$  from a source dataset with overhead  $\mathcal{S}$ , where  $\mathbb{D} = \{I_i, T_i\}_{i=1}^N$  comprises  $N$  image-caption pairs. And then optimize model  $\Theta$  on vision-language pre-training task  $\mathcal{L}$ , thereby maximizing general performance  $\mathcal{A}$ . While  $\mathcal{A}$  is challenging to verify on a given vision-language model, it can be inferred through diverse abilities such as visual recognition and compositional reasoning, with evaluation tools like VLMEvalKit [17]. Mathematically  $\mathbb{V} = \Psi(\mathbb{D})$ , and  $\Psi$  can be obtained as

$$\arg \max_{\Psi} \mathcal{A}(\arg \min_{\Theta} \mathcal{L}(\Theta, \mathcal{T}, \Psi)), \quad (1)$$

There are various options to define  $\mathcal{T}$ ,  $\mathcal{S}$ ,  $\mathcal{A}$  and  $\mathcal{L}$ . In this work, we define the training budget  $\mathcal{T}$  as the number of pre-trained tokens, and overhead  $\mathcal{S}$  as the time investment in data construction. The pre-training objective  $\mathcal{L}$  is decided by VLP

(InfoNCE, Sigmoid, Caption Loss, etc [62, 81, 84]). And the vision-language model’s performance  $\mathcal{A}$  as the evaluation across different tasks using the VLMEvalKit framework.

**Motivation.** Although images  $I$  and texts  $T$  appear symmetrical, they differ in underlying semantic structures. Images consist of abundant pixels that convey precise semantics, where many patches contribute little to the overall meaning and can be discarded. In contrast, text is organized concisely, but its semantics are often vague and prone to disruption by noise. While DataSieve overlooks the semantic discrepancy which hinders vision-language pretraining. This observation motivates us to design a finer-grained data governor which can effectively balance both modalities, *i.e.*, reduce image redundancy and enhance text semantics, thus improving data quality and facilitating more efficient training.

**Pipeline Overview.** Our data governance consists of two parallel branches in Fig. 2, named **vision branch** and **text branch**. The vision branch reduces redundancy by discarding semantically insignificant image patches and assesses the probability of object presence within the scene. This process effectively discretizes image semantics. The text branch then leverages visual objects as guidance for caption enhancement, achieving greater clarity and precision. Through these two branches, we generate a modified dataset  $\mathbb{V}$  comprising image-text pairs that are less redundant and better aligned. Pretrained models  $\Theta$  are subsequently applied to various downstream tasks, whose performances serve as a measure of the effectiveness of the data governor.

#### 3.2. Data Juicer: Condensation & Enhancement

We aim to reduce image redundancy at the patch level and improve cross-modal consistency. Given a dataset  $\mathbb{D} = (I_i, T_i)_{i=1}^N$ , where  $(I, T)$  represents a raw image-text pair,

we first patch the image  $I$  to remove redundant patches and then enhance the text  $T$  with visual semantics from  $I$ . The vision and text branches are outlined as follows.

**The Vision Branch** reduces image patch redundancy by evaluating each patch’s contribution to the overall semantics, using similarity scores to identify and discard insignificant patches. Specifically, the vision governor  $\Psi_{\text{img}}$  eliminates patches whose embeddings significantly diverge from the [CLS] embedding, which encapsulates the image’s global semantics. By removing patches with low similarity to the [CLS] embedding, redundancy is effectively reduced. Additionally, the class prediction derived from the [CLS] embedding provides object existence probabilities, guiding the enhancement of textual descriptions.

With image  $I \in \mathbb{R}^{H \times W}$  split into  $m$  patches  $\{I_t\}_{t=1}^m \in \mathbb{R}^{m \times B}$ , each of  $B = HW/m^2$  pixels.  $\Psi_{\text{img}}$  scores and selects patches with its last-layer attention mechanism. We initialize  $\Psi_{\text{img}}$  with DINO [4], and denote  $\mathbf{W}_Q, \mathbf{W}_K \in \mathbb{R}^{d_k}$  as query, key matrix. From previous layer, there are corresponding visual tokens  $\{\mathbf{v}_t\}_{t=1}^m \in \mathbb{R}^{m \times d}$ , and a special [CLS] token  $\mathbf{v}_c \in \mathbb{R}^d$  representing the overall feature of  $I$ . The contribution scores  $\mathbf{s} \in \mathbb{R}^m$  of the image patches  $I_t$  are determined by

$$\mathbf{s} = \frac{(\mathbf{v}_c \mathbf{W}_Q)([\mathbf{v}_1, \dots, \mathbf{v}_m] \mathbf{W}_K)^T}{\sqrt{d_k}} \quad (2)$$

Thus the top- $k$  patches are retained because of the most contribution to the global visual embedding  $\mathbf{v}_c$ . While the others, contributing less to the overall semantics, are discarded. This reduction in visual tokens reduces the computational cost during VLP. The resulting image is represented as:

$$I' = \{I_t\}_{t=1}^k \in \mathbb{R}^{k \times B}. \quad (3)$$

Given the image embedding  $\mathbf{v}_c$ , the vision governor  $\Psi_{\text{img}}$  predicts  $L$  class labels  $C$  of the image  $I$  using a class prediction head,  $\Gamma_{\text{pred}}$  initialized from DINO. The object existence probabilities are represented as  $\mathbf{p} \in \mathbb{R}^L$ .

$$\mathbf{p} = \Gamma_{\text{pred}}(\mathbf{v}_c). \quad (4)$$

*Remark.* In the vision branch, Vision FMs can offer us free knowledge about data requiring no extra computation cost. The vision governor reduces redundancy by discarding noisy, insignificant patches while retaining the most informative ones. As a result, the new image  $I'$  is of higher quality and less computation for  $\Theta$  pretraining. Furthermore, the class prediction process transforms redundant visual semantics into discrete object classes, offering clear visual evidence for the text branch’s further enhancement.

**The Text Branch.** To mitigate the noise impact in input texts, the text governor  $\Psi_{\text{txt}}$  enhances and denoises texts  $T$  with the assistance of visual semantics.  $\Psi_{\text{txt}}$  is one Large

Language Model, such as LLaMA [72], Qwen [2], and we construct the prompts  $P_O$ , incorporating class names given by  $\mathbf{p}$  from Equ. 4. As the distribution of  $\mathbf{p}$  indicates the confidence of class predictions, we set a threshold  $\epsilon$  and only take classes of  $\mathbf{p} > \epsilon$  into  $P_O$  construction, denoted as  $C'$ .

As texts  $T$  may contain imperfections like misspellings and repetitive expressions, the text governor  $\Psi_{\text{txt}}$  leverages contextual information to denoise the text. It constructs a textual correction prompt  $P_M$  and combine it with the visual correction prompt  $P_O$ . As a result,  $\Psi_{\text{txt}}$  uses both  $P_M$  and  $P_O$  as prompts, to correct the imperfections in  $T$ , thereby generating new caption  $T'$ .

$$T'_i = \Psi_{\text{txt}}(P_M, P_O, T_i). \quad (5)$$

Combining the efforts of both vision and text branches, we get new training data

$$\mathbb{V} = \{I'_i, T'_i\}_{i=1}^N. \quad (6)$$

*Remark.* In the text branch, we use the LLMs to enhance and denoise the text data: (1) *Enhancement:* Incorporating visual evidences  $C'$  from the vision branch  $\Psi_{\text{img}}$  is challenging, due to the absence of direct mapping from  $C'$  to raw caption components in  $T$ . LLMs  $\Psi_{\text{txt}}$ , leveraging inherent world knowledge, infer the linking from visual evidence to caption components, thereby enhancing the captions. (2) *Denoising:* Web-sourced texts are often informal and grammatically lax, rendering them unsuitable for image descriptions. The text governor  $\Psi_{\text{txt}}$  performs textual correction to eliminate errors such as misspellings and repetitive expressions to improve the captions’ quality.

To conclude, with the vision and text branch combined, we obtain a more compact dataset, which has less noise and improved image-caption consistency.

### 3.3. Vision-Language Pre-Training

Given the governed dataset  $\mathbb{V}$ , we train vision-language models  $\Theta$  from scratch. We describe the architecture first and then introduce the training objectives.

**Architecture.** Given  $\mathbb{V} = (I'_i, T'_i)_{i=1}^N$  as image-text training pairs, the vision-language pretraining models  $\Theta$  typically comprises an image encoder  $\Theta_{\text{img}}$  and a text encoder  $\Theta_{\text{txt}}$ . We use CLIP [62] for demonstration.

In detail, we encode a specific image-text pair  $(I, T)$  separately with the image/text encoder  $\Theta_{\text{img}/\text{txt}}$ , the embedding dimension is denoted as  $d$ :

$$\mathbf{v}'_{\text{img}} = \Theta_{\text{img}}(I') \in \mathbb{R}^d, \quad (7)$$

$$\mathbf{v}'_{\text{txt}} = \Theta_{\text{txt}}(T') \in \mathbb{R}^d, \quad (8)$$

where  $\mathbf{v}'_{\text{img}}$  represents the embedding for the image, and  $\mathbf{v}'_{\text{txt}}$  refers to the text embedding.

**Image-Text Contrastive Learning (ITC).** We implement ITC loss following CLIP [62], which aligns the corresponding visual and textual representations for each sample in a batch. In detail, denoting batch size as  $b$ , we calculate the softmax-normalized cross-modality dot product similarity between the current visual/text embedding ( $v'_{\text{img}}/v'_{\text{txt}}$ ) and all samples within the batch, termed as  $p^{i2t}, p^{t2i} \in \mathbb{R}^b$ , and the final ITC loss is formulated as:

$$\mathcal{L}_{\text{ITC}} = \mathbb{E}_{(I,T) \sim \mathbb{V}} [\text{CE}(y^{i2t}, p^{i2t}) + \text{CE}(y^{t2i}, p^{t2i})], \quad (9)$$

where  $y^{i2t}, y^{t2i}$  refer to one-hot matching labels, and CE refers to the InfoNCE loss [24].

**Train & Inference.** While image patches used during training and inference differ, our framework is flexible and requires no modifications for downstream tasks. The vision-language model is pre-trained on a subset of image patches, yet it can be directly applied to complete images during inference. This straightforward setup yields competitive performance on downstream tasks and serves as a baseline for our ablation experiments.

Using a subset of image patches as input during inference is also allowed. The patch reduction creates a trade-off between inference speed and performance. For downstream tasks requiring only coarse-grained visual semantics, they can use fewer patches as input for inference acceleration.

## 4. Experiment

### 4.1. Datasets & Implementation Details

**Training Datasets.** CC3M [65] and CC12M [5] are widely used vision-language pre-training datasets. They gather massive web-sourced images and alt-texts, then perform simple data cleansing, *e.g.*, image filtering by resolution, and text cleaning by length. Despite their vast scale and rich diversity, unhelpful or even detrimental samples persist. YFCC15M [62], a 15M subset of the multilingual and noisy YFCC100M [68] that contains English captions, is also used to validate DataJuicer’s generalizability to data in the wild. LAION400M [63] is an even larger noisy dataset for VLP. To reduce the computation cost and storage overhead, we randomly sample LAION40M from LAION400M.

**Testing Datasets & Metrics.** For image-text retrieval, MSCOCO [41] and Flickr30 [80] are used as standard benchmarks. For image classification, we utilize the ImageNet [16](ImgN1K/-R/-A) validation set. To demonstrate how DataJuicer-enhanced data improves visual encoder, We replace LLaVA-13B [43]’s vision backbone with our image encoder pretrained on refined datasets  $\mathbb{V}$  for comprehensive evaluation. We follow conventions to evaluate with consensus metrics: using Top-1/5 accuracy for classification; R@1/5/10 for image-text retrieval; and follow [17] to evaluate LLaVA on [20, 23, 38, 48, 51, 58, 64, 66, 82]. Note that all testing are standardized to ensure fairness.

**Implementation** We utilize PyTorch [60] to implement our models and train them on 8 NVIDIA A100 GPUs. The model is pre-trained for 50 epochs with a batch size of 1024 and an AdamW [50] optimizer with a weight decay of 0.05. During training, we apply a learning rate warm-up to 3e-4 and OneCycle scheduler (cosine annealing) [49]. All images were cropped to a resolution of  $224 \times 224$  during training and inference. More training hyperparameters for downstream tasks are put in the supplementary materials.

### 4.2. Comparison with SoTA Methods

**Performance Comparisons.** Tab. 2 compares our DataJuicer with coarse and fine-grained data governing methods on image-text retrieval (COCO, Flickr), image classification (ImgN1K, ImgNR, ImgNA) and MLLM downstream tasks (OKVQA, CCBench, etc). In the first part, we introduce DataSieve, whose simplest baseline is random selection before training. Clip-score, as a classical metric for image-text correspondence estimation, is used to decide whether to retain samples. An alternative baseline clusters the dataset into subsets and enforces uniform sampling across all groups. To make a wider comparison, we include 4 SoTA sample selection methods [1, 56, 70, 73]. These methods select the most representative samples leveraging embeddings from pre-trained models, via heuristic sampling procedures. Then we introduce fine-grained governing methods in the second part. Rather than sample-wise selection based on heuristic metrics, fine-grained data governors refine dataset at the token level. Thus the token-wise Random\*/Cluster\* approaches produce training samples with higher information density compared to those generated by coarse-grained Random/Cluster operations. Therefore, as shown in Tab. 2, Random\*/Cluster\* usually performs better than Random/Cluster and many coarse-grained methods.

From Tab. 2, we obtain two observations: 1). DataJuicer shows a clear gain compared to competitors on most downstream tasks; 2). Fine-grained methods outperform coarse-grained ones even without well-designed sampling.

**Efficiency Comparisons.** We also compare efficiency between DataJuicer and other methods. Although the motivations of these methods are diverse, their main goal is to save training costs. Thus, we report training time of  $\Theta$ , overhead used for  $\mathbb{V}$  dataset curation, and total GPU hours of these methods in Tab. 3. Previous sieving-based methods discard unworthy samples while ignoring token-wise redundancy. DataJuicer wisely spends computation on most informative tokens told by vision foundation models, further reducing token redundancy. More importantly, DataJuicer achieves both faster inference and superior performance on ImageNet-1K at the image retention ratio  $r = k/m = 0.5$ . To explore the joint impact of DataJuicer and DataSieve, DataJuicer×Sieve applies DataJuicer on DataSieve’s retained samples. Such one combination further enhances performance and effi-

Table 2. **Comparison to State-of-The-Art Methods.** All methods set compression ratios to 50% and train CLIP from scratch for fairness. We describe sample-sieving methods as coarse-grained and token-juicing ones as fine-grained. Full Data refers to results without data governance. More implementation details are available in Appendix A.

	Method	COCO	Flickr	ImgN1K	ImgNR	ImgNA	OKVQA	CCBench	HaBench	MMBench	MMMU	MMStar	POPE
Coarse	Full Data	11.68	26.2	17.71	19.56	4.32	62.00	1.18	35.64	42.35	37.33	26.00	77.84
	Random	6.18	14.7	11.28	11.99	2.52	57.11	2.33	35.43	40.63	29.30	23.20	76.02
	Cluster	6.58	14.6	11.28	12.08	2.56	59.56	2.15	34.06	38.83	29.30	22.66	<b>80.17</b>
	CLIP-Score	6.60	14.2	11.57	13.53	2.89	62.53	1.17	36.27	38.23	28.60	24.20	78.31
	D2Pruning [56]	7.43	16.4	11.58	12.22	3.65	54.42	1.40	31.00	37.88	28.00	23.35	79.43
	TLDR [73]	9.66	21.4	11.88	14.79	3.28	57.9	1.18	31.96	37.20	<b>29.33</b>	22.80	79.78
	SemDeDup [1]	7.06	16.4	11.55	12.64	3.40	54.23	1.37	31.54	37.28	28.00	23.46	79.51
	D4 [70]	8.83	17.9	12.25	14.12	3.93	55.88	2.69	31.59	37.93	28.30	23.30	77.16
Fine	Random*	9.14	21.2	14.02	15.94	3.61	57.55	2.35	36.06	38.91	29.00	24.13	77.53
	Cluster*	9.42	21.4	14.86	16.08	3.56	57.86	2.43	36.21	38.67	28.70	24.50	77.29
	<b>DataJuicer</b>	<b>9.72</b>	<b>21.8</b>	<b>15.54</b>	<b>17.32</b>	<b>4.00</b>	<b>62.10</b>	<b>3.52</b>	<b>36.91</b>	<b>42.78</b>	<b>29.33</b>	<b>27.07</b>	77.26

Table 3. **Training Efficiency Comparison.** Results are reported on ImageNet-1K with CLIP under 50% prune ratio on an 8-A100 GPU server. DataJuicer×Sieve applies DataJuicer on retained samples from DataSieve. Total computation costs are calculated by GPU hours (n\*h). Our default settings are marked in blue.

Method	Acc	Time	Overhead	Total (n*h)
Full Data	17.7	27	-	216.1
TLDR	11.9	14	1.2	113.2
D4	12.6	14	1.2	113.2
SemDeDup	11.6	14	1.2	113.2
<b>DataJuicer</b>	<b>15.5</b>	<b>13</b>	<b>0.8</b>	<b>104.8</b>
<b>DataJuicer</b> ×Sieve	<b>15.7</b>	14	2.5	114.5

ciency, thereby confirming DataJuicer’s complementary role in data governance alongside DataSieve.

We show the inference efficiency of DataJuicer in Tab. 4. Finer-grained token view reduces computation cost per sample, therefore DataJuicer exhibits faster speed on equal-sized samples compared to DataSieve. Reducing the retention ratio  $r = k/m$  further accelerates inference while incurring a performance trade-off. This paper sets  $r = 1.0$  by default, while users may adjust it by need.

### 4.3. Scaling Behavior

To match the extensive training scale of foundation models, we compare scaling behavior between DataJuicer and DataSieve. We demonstrate DataJuicer’s superior potential along either of these three axes:

- **Data Scaling.** We scale pre-training data from 3 to 12 million, using the CC12M set [5]. To better ablate the training efficiency of DataJuicer over DataSieve, we align data governors under the same token expenses.
- **Model Scaling.** We scale from CLIP-S to CLIP-L, which has around  $10\times$  parameters.
- **Schedule Scaling.** We increase the sampled token from 30 to 80G (50 epochs of 12M data).

Fig. 3 studies scaling along one of these three axes at each time while keeping others unchanged.

*Data Scaling.* In Fig. 3 Left, we scale up the training size from 3M to 12M on CLIP (ViT-Base, BERT-Base), and

Table 4. **Inference Efficiency Comparison.** With image retention ratio  $r = \frac{k}{m} = 0.5$ , our DataJuicer exhibits faster inference on equal-sized samples compared to DataSieve. We report Top-1 accuracy (acc) on ImageNet-1K and fp32 CLIP (ViT-B/16, BERT-Base) throughput (im/s) on a V100 GPU.

Method	Acc	GFlops	Im/s	Speed
TLDR	11.9	13.2	158	1×
D4	12.3	13.2	158	1×
SemDeDup	11.6	13.2	158	1×
<b>DataJuicer</b> <sub><math>r=1.0</math></sub>	<b>15.5</b>	13.2	158	1×
<b>DataJuicer</b> <sub><math>r=.50</math></sub>	15.4	7.7	191	1.7×
<b>DataJuicer</b> <sub><math>r=.25</math></sub>	13.4	<b>4.8</b>	<b>585</b>	<b>3.7×</b>

compare performances of models trained on data generated by DataJuicer and DataSieve respectively. The x-axis is the quantity of sampled tokens during training, and the y-axis is the zero-shot accuracy on ImageNet-1K. Note that with equivalent token sampling volumes, DataJuicer costs less computation while achieving better performance. A clear gap persists throughout training, suggesting DataJuicer’s wiser computation investment on informative tokens. With higher per-token marginal returns, DataJuicer makes a more suitable data governor than DataSieves under data scaling.

*Model Scaling.* Fig. 3 Middle presents data governors’ model scaling behavior, showing that DataJuicers perform superior than DataSieve on larger models. While the increase in model size enhances performance, model scaling exacerbates inherent limitations in training data, thus imposing heightened demands in data governance. Modern MLLMs favor larger image encoders to push through the visual capability bottleneck. Therefore, the superior performance of DataJuicer over DataSieve underscores its advantage in supporting advanced foundation models. The model configurations of ViT-S/B/L are detailed in Appendix A.

*Schedule Scaling.* Fig. 3 Right trains longer given the same curated dataset  $\mathbb{V}$  and model  $\Theta$ . The gain brought by DataJuicer is amplified as the sampled data increases.

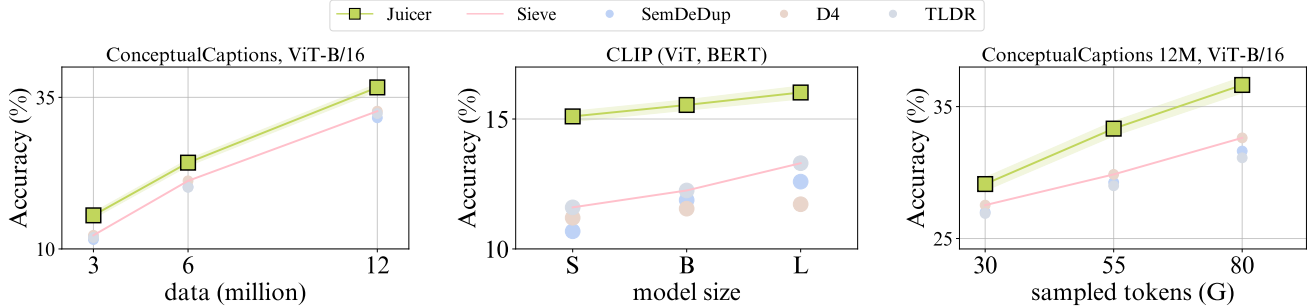


Figure 3. The highest DataSieve results are marked in pink. **Data Scaling** (Left). With training data scaled from CC3M to CC12M, a clear gap persists throughout training, suggesting DataJuicer’s wiser computation investment on informative tokens. **Model Scaling** (Middle). DataJuicer outperforms DataSieve across CLIP sizes (from S to L), showing large VLP models also learn better on juiced data. **Schedule Scaling** (Right). We train the same CLIP longer up to 82G sampled tokens (epochs of 12M data).

#### 4.4. Generalization Evaluation

**Cross-data Evaluation.** To validate the generalization efficacy for data governors, we evaluate across various datasets for VLP. Unprocessed datasets  $\mathbb{D}$  are classified into two categories, clean data filtered with human intervention and web-sourced wild data without cleaning. Well-cleaned, high-quality examples of the former include CC3M and CC12M, while subsets YFCC15M (from YFCC100M) and LAION40M (from LAION400M) are wild data exemplars.

We use CLIP as the default architecture and evaluate on MSCOCO, ImageNet-1K and MMStar, three representative benchmarks in retrieval, classification and MLLM tasks. As observed in Fig. 4, DataJuicer outperforms DataSieves across various training data. The gains on YFCC15M and LAION40M prove the DataJuicer’s effectiveness on noisy data sourced from the web.

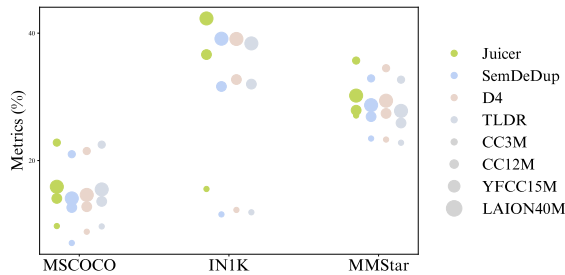


Figure 4. **Generalization Across Data.** DataJuicer performs better on both well-cleaned datasets and larger noisy datasets (larger markers). We choose one typical benchmark from each downstream task, *i.e.*, MSCOCO for retrieval, ImageNet-1K for classification and MMStar for MLLM evaluation.

**Cross-architecture Evaluation.** For vision-language pre-training, there are various models that are broadly adopted [79]. These models splits images into patches and embeds these into token sequences, enabling them to leverage the finer-grained data governor. As in Fig 5, we ap-

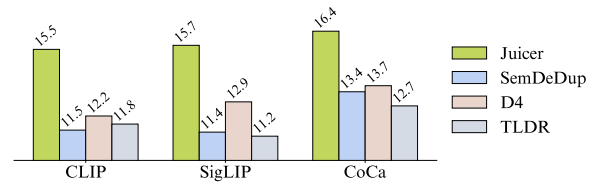


Figure 5. **Generalization Across Architectures.** For fair comparison, we train models with tokens of equal size, and then report zero-shot performances on ImageNet-1K.

ply DataJuicer to 3 famous model architectures (CLIP [62], SigLIP [84], CoCa [81]), where DataJuicer achieves superior performance than DataSieve across all of them. Therefore we justify DataJuicer’s cross-architecture generalization.

#### 4.5. Ablation Studies

We perform extensive ablations to dissect designs of DataJuicer. If not stated, experiments use CC3M as the original dataset and conduct a zero-shot evaluation on ImageNet-1K.

Patch contributions are quantified based on the contributions of their corresponding tokens to the overall semantics encoded by ViT. Pretrained ViT from DINO-S best balances performance and inference speed (Tab. 5a). Despite CLIP’s competitive performance, we opt for vision-only foundation models (*e.g.* DINO, MAE) to insulate patch contribution estimation from text interference.

Patch selection applies sampling on scored image patches and forwards chosen ones for training. Stratified sampling selects from patch partitions of different scores and performs slightly better than other sampling (Tab. 5b). We use topk selection as default to keep the selection user-friendly.

The image patch size decides the granularity of DataJuicer, with smaller patches enabling more precise selection. As shown in Tab. 5c, models trained with images of smaller patches benefit even more from DataJuicer.

Confidence threshold  $\epsilon$  is set to extract high-certainty visual evidence from images. As in Tab. 5d, we set the

Model	Top1	Im/s
CLIP	<b>16.72</b>	158.2
DINO-S	15.54	<b>393.4</b>
DINO-B	15.58	259.3
DINOv2-L	15.86	190.2

(a) **Patch Contribution.** We choose DINO-S to balance performance and computing overhead during data governance.

Thresh ( $\epsilon$ )	Top1	Top5
50%	15.03	31.37
70%	<b>15.54</b>	<b>31.74</b>
90%	14.73	30.54

(d) **Confidence Thresh** should maintain sufficient visual evidence while minimizing noise.

Method	Top1	Top5
uniform	13.47	28.26
topk	15.54	<b>31.74</b>
stratified	<b>15.61</b>	31.28
mix	15.47	31.17

(b) **Patch Selection.** In fact, stratified sampling achieves comparable performances, while we use topk as default for simplicity.

Method	Top1	Top5
none	11.28	24.54
text-only	12.76	26.12
concat	15.31	31.56
rewrite	<b>15.54</b>	<b>31.74</b>

(e) **Caption Enhancement.** Incorporating visual evidence (see Eq. 4) improves accuracy.

Size	Acc	Im/s
32	15.47	<b>407.5</b>
16	<b>15.54</b>	393.4
14	<b>15.94</b>	335.6

(c) **Patch Size.** Smaller patches enable more precise patch selection and finer-grained data governance.

Step	$\mathcal{T}$ (%)	Top1
0	0	15.54
2%	4 $\uparrow$	16.02
4%	8 $\uparrow$	16.35
8%	16 $\uparrow$	<b>16.72</b>

(f) **Full-Patch Tuning** mitigates the train/infer gap but incurs  $\mathcal{T}\%$  compute budget.

Table 5. **DataJuicer Ablation Experiments** use CLIP trained on curated dataset  $\mathbb{V}$ , and use ImageNet-1k for zero-shot evaluation. We report Top-1/5 accuracy and fp32 model throughput (im/s) on a V100 GPU. Our default settings are marked in purple.

confidence thresh  $\epsilon = 0.7$  to avoid compromising caption accuracy. Users can choose a moderately relaxed threshold to merge more visual semantics to enhance captions.

Caption enhancement incorporates visual semantics from DataJuicer’s vision branch to refine and enrich captions with LLM, thereby improving image-caption alignment. DataJuicer degenerates to vision-only data governor when none caption enhancement applied. Comparison against text-only enhancement and direct object name concatenation demonstrates the benefits of LLM rewrite (Tab. 5e).

Full-patch tuning involves all image patches during the late training phase. Tab. 5f shows that full-patch tuning on last epoch alone can benefit performance on fine-grained visual recognition (e.g. POPE), costing only 2% extra computational overhead. While it is excluded by default for a fair comparison with DataSieve, this idea remains optional for users, to incur tasks demanding all image details.

## 4.6. Visualizations

Fig. 6 illustrates some modified samples generated by DataJuicer, where significant patches are removed through **patch selection** and masked with gray regions. Real-world text descriptions often exhibit imperfections, vague descriptions of objects, omission of key elements, non-descriptive expressions, etc. We demonstrate **caption enhancement** as follows: (1) *Top*: The key elements ‘Steam Locomotive, Lakeshore’ are omitted in the original caption. DataJuicer utilizes LLM to infer the scene given the original text and objects predicted from Vision FMs, effectively reconstructing the image’s context. (2) *Bottom*: A significant portion of web images are shared to convey experiences, where the captions are complementary semantics of images (e.g. ‘stupa’ in the image and ‘team’ in the caption), resulting in weak correspondence between the image and the original caption. DataJuicer integrates image semantics with the original caption to form a complete description of the scene.

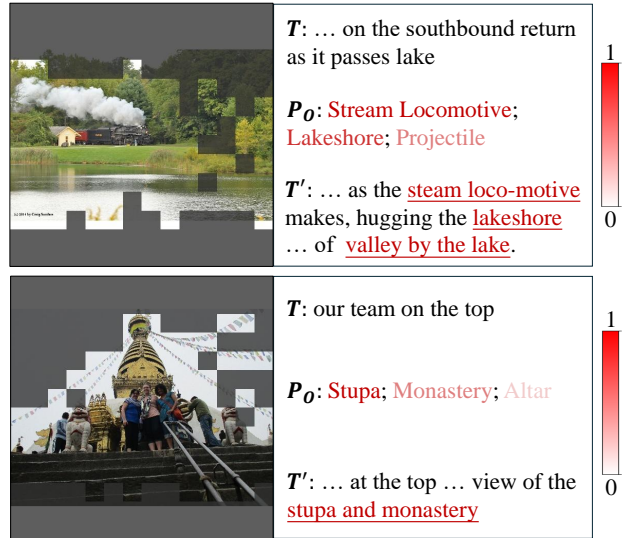


Figure 6. DataJuicer reduce visual redundancy by discarding less contributive 50% image patches as masked in visualization. We mark visual evidence  $P_O$  in red from dark to light based on their confidence. More visualizations are to be found in Appendix B.

Accordingly, it is concluded that DataJuicer deals with data redundancy and noise effectively.

## 5. Conclusion

The paper presents DataJuicer as a novel approach as data governance. By employing a token view, we significantly improve the data quality and model performance. With rigorous experiments and massive ablations, our framework shows superior performance in image-text retrieval, classification and a range of dense visual tasks, surpassing DataSieve with substantial improvements. This paper emphasizes the vital advantage of DataJuicer for finer-grained data governor, paving the way for future progress in data governance.



## References

- [1] Amro Abbas, Kushal Tirumala, Dániel Simig, Surya Ganguli, and Ari S. Morcos. Semdedup: Data-efficient learning at web-scale through semantic deduplication, 2023. 1, 2, 5, 6
- [2] Jinze Bai, Shuai Bai, Shusheng Yang, Shijie Wang, Sinan Tan, Peng Wang, Junyang Lin, Chang Zhou, and Jingren Zhou. Qwen-vl: A frontier large vision-language model with versatile abilities. *arXiv preprint arXiv:2308.12966*, 2023. 1, 4
- [3] Seth Baum. A survey of artificial general intelligence projects for ethics, risk, and policy. *Global catastrophic risk institute working paper*, pages 17–1, 2017. 1
- [4] Mathilde Caron, Hugo Touvron, Ishan Misra, Hervé Jégou, Julien Mairal, Piotr Bojanowski, and Armand Joulin. Emerging properties in self-supervised vision transformers. In *Proceedings of the IEEE/CVF international conference on computer vision*, pages 9650–9660, 2021. 2, 4
- [5] Soravit Changpinyo, Piyush Sharma, Nan Ding, and Radu Soricut. Conceptual 12M: Pushing web-scale image-text pre-training to recognize long-tail visual concepts. In *CVPR*, 2021. 5, 6
- [6] Mengting Chen, Xi Chen, Zhonghua Zhai, Chen Ju, Xuewen Hong, Jinsong Lan, and Shuai Xiao. Wear-any-way: Manipulable virtual try-on via sparse correspondence alignment. In *European Conference on Computer Vision*. Springer, 2024. 2
- [7] Shaoxiang Chen, Wenhao Jiang, Wei Liu, and Yu-Gang Jiang. Learning modality interaction for temporal sentence localization and event captioning in videos. In *Proceedings of the European Conference on Computer Vision*. Springer, 2020. 2
- [8] Xu Chen, Zida Cheng, Jiangchao Yao, Chen Ju, Weilin Huang, Jinsong Lan, Xiaoyi Zeng, and Shuai Xiao. Enhancing cross-domain click-through rate prediction via explicit feature augmentation. In *International World Wide Web Conference*, 2024. 2
- [9] Yen-Chun Chen, Linjie Li, Licheng Yu, Ahmed El Kholy, Faisal Ahmed, Zhe Gan, Yu Cheng, and Jingjing Liu. Uniter: Universal image-text representation learning. In *Proceedings of the European Conference on Computer Vision*. Springer, 2020. 2
- [10] Zhe Chen, Jiannan Wu, Wenhao Wang, Weijie Su, Guo Chen, Sen Xing, Muyan Zhong, Qinglong Zhang, Xizhou Zhu, Lewei Lu, et al. Internvl: Scaling up vision foundation models and aligning for generic visual-linguistic tasks. In *Proceedings of the IEEE/CVF Conference on Computer Vision and Pattern Recognition*, pages 24185–24198, 2024. 1
- [11] Feng Cheng, Xizi Wang, Jie Lei, David Crandall, Mohit Bansal, and Gedas Bertasius. Vindlu: A recipe for effective video-and-language pretraining. In *Proceedings of the IEEE Conference on Computer Vision and Pattern Recognition*, 2023. 2
- [12] Haozhe Cheng, Cheng Ju, Haicheng Wang, Jinxiang Liu, Mengting Chen, Qiang Hu, Xiaoyun Zhang, and Yanfeng Wang. Denoiser: Rethinking the robustness for open-vocabulary action recognition. *arXiv preprint arXiv:2404.14890*, 2024. 2
- [13] Zida Cheng, Chen Ju, Xu Chen, Zhonghua Zhai, Shuai Xiao, Xiaoyi Zeng, and Weilin Huang. Image to multi-modal retrieval for industrial scenarios. *arXiv preprint arXiv:2305.03972*, 2023. 2
- [14] Zida Cheng, Chen Ju, Shuai Xiao, Xu Chen, Zhonghua Zhai, Xiaoyi Zeng, Weilin Huang, and Junchi Yan. Category-oriented representation learning for image to multi-modal retrieval. *arXiv preprint arXiv:2305.03972*, 2023. 2
- [15] Zida Cheng, Shuai Xiao, Zhonghua Zhai, Xiaoyi Zeng, and Weilin Huang. Mixer: Image to multi-modal retrieval learning for industrial application. *arXiv preprint arXiv:2305.03972*, 2023. 2
- [16] Jia Deng, Wei Dong, Richard Socher, Li-Jia Li, Kai Li, and Li Fei-Fei. Imagenet: A large-scale hierarchical image database. In *2009 IEEE conference on computer vision and pattern recognition*, pages 248–255. Ieee, 2009. 5
- [17] Haodong Duan, Junming Yang, Yuxuan Qiao, Xinyu Fang, Lin Chen, Yuan Liu, Xiaoyi Dong, Yuhang Zang, Pan Zhang, Jiaqi Wang, et al. Vlmevalkit: An open-source toolkit for evaluating large multi-modality models. *arXiv preprint arXiv:2407.11691*, 2024. 3, 5
- [18] Lijie Fan, Dilip Krishnan, Phillip Isola, Dina Katabi, and Yonglong Tian. Improving clip training with language rewrites. *Advances in Neural Information Processing Systems*, 2024. 3
- [19] Chengjian Feng, Yujie Zhong, Zequn Jie, Xiangxiang Chu, Haibing Ren, Xiaolin Wei, Weidi Xie, and Lin Ma. Promptdet: Towards open-vocabulary detection using uncurated images. In *European Conference on Computer Vision*, pages 701–717. Springer, 2022. 2
- [20] Chaoyou Fu, Peixian Chen, Yunhang Shen, Yulei Qin, Mengdan Zhang, Xu Lin, Jinrui Yang, Xiawu Zheng, Ke Li, Xing Sun, et al. Mme: A comprehensive evaluation benchmark for multimodal large language models. *arXiv preprint arXiv:2306.13394*, 2023. 5
- [21] Ben Goertzel. Artificial general intelligence: concept, state of the art, and future prospects. *Journal of Artificial General Intelligence*, 5(1):1, 2014. 1
- [22] Sachin Goyal, Pratyush Maini, Zachary C Lipton, Aditi Raghunathan, and J Zico Kolter. Scaling laws for data filtering—data curation cannot be compute agnostic. In *Proceedings of the IEEE/CVF Conference on Computer Vision and Pattern Recognition*, pages 22702–22711, 2024. 2
- [23] Tianrui Guan, Fuxiao Liu, Xiyang Wu, Ruiqi Xian, Zongxia Li, Xiaoyu Liu, Xijun Wang, Lichang Chen, Furong Huang, Yaser Yacoob, Dinesh Manocha, and Tianyi Zhou. Hallusionbench: An advanced diagnostic suite for entangled language hallucination and visual illusion in large vision-language models. In *Proceedings of the IEEE/CVF Conference on Computer Vision and Pattern Recognition (CVPR)*, pages 14375–14385, 2024. 5
- [24] Kaiming He, Haoqi Fan, Yuxin Wu, Saining Xie, and Ross Girshick. Momentum contrast for unsupervised visual representation learning. In *Proceedings of the IEEE/CVF conference on computer vision and pattern recognition*, 2020. 5
- [25] Jonathan Ho, Ajay Jain, and Pieter Abbeel. Denoising diffusion probabilistic models. *Advances in Neural Information Processing Systems*, 2020. 1
- [26] Chao Jia, Yinfei Yang, Ye Xia, Yi-Ting Chen, Zarana Parekh, Hieu Pham, Quoc Le, Yun-Hsuan Sung, Zhen Li, and Tom

- Duerig. Scaling up visual and vision-language representation learning with noisy text supervision. In *International conference on machine learning*, pages 4904–4916. PMLR, 2021. 1, 2
- [27] Chen Ju, Peisen Zhao, Ya Zhang, Yanfeng Wang, and Qi Tian. Point-level temporal action localization: Bridging fully-supervised proposals to weakly-supervised losses. *arXiv preprint arXiv:2012.08236*, 2020. 2
- [28] Chen Ju, Peisen Zhao, Siheng Chen, Ya Zhang, Yanfeng Wang, and Qi Tian. Divide and conquer for single-frame temporal action localization. In *Proceedings of the International Conference on Computer Vision*, 2021. 2
- [29] Chen Ju, Tengda Han, Kunhao Zheng, Ya Zhang, and Weidi Xie. Prompting visual-language models for efficient video understanding. In *Proceedings of the European Conference on Computer Vision*. Springer, 2022. 2
- [30] Chen Ju, Peisen Zhao, Siheng Chen, Ya Zhang, Xiaoyun Zhang, Yanfeng Wang, and Qi Tian. Adaptive mutual supervision for weakly-supervised temporal action localization. *IEEE Transactions on Multimedia*, 2022. 2
- [31] Chen Ju, Zeqian Li, Peisen Zhao, Ya Zhang, Xiaopeng Zhang, Qi Tian, Yanfeng Wang, and Weidi Xie. Multi-modal prompting for low-shot temporal action localization. *arXiv preprint arXiv:2303.11732*, 2023. 2
- [32] Chen Ju, Haicheng Wang, Zeqian Li, Xu Chen, Zhonghua Zhai, Weilin Huang, and Shuai Xiao. Turbo: Informativity-driven acceleration plug-in for vision-language models. *arXiv preprint arXiv:2312.07408*, 2023. 2
- [33] Chen Ju, Haicheng Wang, Jinxiang Liu, Chaofan Ma, Ya Zhang, Peisen Zhao, Jianlong Chang, and Qi Tian. Constraint and union for partially-supervised temporal sentence grounding. *arXiv preprint arXiv:2302.09850*, 2023. 2
- [34] Chen Ju, Kunhao Zheng, Jinxiang Liu, Peisen Zhao, Ya Zhang, Jianlong Chang, Qi Tian, and Yanfeng Wang. Distilling vision-language pre-training to collaborate with weakly-supervised temporal action localization. In *Proceedings of the IEEE Conference on Computer Vision and Pattern Recognition*, 2023. 2
- [35] Chen Ju, Haicheng Wang, Haozhe Cheng, Xu Chen, Zhonghua Zhai, Weilin Huang, Jinsong Lan, Shuai Xiao, and Bo Zheng. Turbo: Informativity-driven acceleration plug-in for vision-language large models. In *Proceedings of the European Conference on Computer Vision*. Springer, 2025. 2
- [36] Wonjae Kim, Bokyung Son, and Ildoo Kim. Vilt: Vision-and-language transformer without convolution or region supervision. In *International conference on machine learning*. PMLR, 2021. 2
- [37] Zhengfeng Lai, Haotian Zhang, Bowen Zhang, Wentao Wu, Haoping Bai, Aleksei Timofeev, Xianzhi Du, Zhe Gan, Jiulong Shan, Chen-Nee Chuah, et al. Veclip: Improving clip training via visual-enriched captions. In *European Conference on Computer Vision*, pages 111–127. Springer, 2025. 3
- [38] Bohao Li, Yuying Ge, Yixiao Ge, Guangzhi Wang, Rui Wang, Ruimao Zhang, and Ying Shan. Seed-bench: Benchmarking multimodal large language models. In *Proceedings of the IEEE/CVF Conference on Computer Vision and Pattern Recognition*, pages 13299–13308, 2024. 5
- [39] Junnan Li, Dongxu Li, Caiming Xiong, and Steven Hoi. Blip: Bootstrapping language-image pre-training for unified vision-language understanding and generation. In *International Conference on Machine Learning*, pages 12888–12900. PMLR, 2022. 2
- [40] Junnan Li, Dongxu Li, Silvio Savarese, and Steven Hoi. Blip-2: Bootstrapping language-image pre-training with frozen image encoders and large language models. *arXiv preprint arXiv:2301.12597*, 2023. 2
- [41] Tsung-Yi Lin, Michael Maire, Serge Belongie, James Hays, Pietro Perona, Deva Ramanan, Piotr Dollár, and C Lawrence Zitnick. Microsoft coco: Common objects in context. In *Computer Vision—ECCV 2014: 13th European Conference, Zurich, Switzerland, September 6–12, 2014, Proceedings, Part V 13*. Springer, 2014. 5
- [42] Weixiong Lin, Ziheng Zhao, Xiaoman Zhang, Chaoyi Wu, Ya Zhang, Yanfeng Wang, and Weidi Xie. Pmc-clip: Contrastive language-image pre-training using biomedical documents. In *International Conference on Medical Image Computing and Computer-Assisted Intervention*, pages 525–536. Springer, 2023. 1, 2
- [43] Haotian Liu, Chunyuan Li, Yuheng Li, and Yong Jae Lee. Improved baselines with visual instruction tuning. In *Proceedings of the IEEE/CVF Conference on Computer Vision and Pattern Recognition*, pages 26296–26306, 2024. 1, 2, 5
- [44] Jinxiang Liu, Chen Ju, Weidi Xie, and Ya Zhang. Exploiting transformation invariance and equivariance for self-supervised sound localisation. In *Proceedings of ACM International Conference on Multimedia*, 2022. 2
- [45] Jinxiang Liu, Chen Ju, Chaofan Ma, Yanfeng Wang, Yu Wang, and Ya Zhang. Audio-aware query-enhanced transformer for audio-visual segmentation. *arXiv preprint arXiv:2307.13236*, 2023. 2
- [46] Jinxiang Liu, Yikun Liu, Fei Zhang, Chen Ju, Ya Zhang, and Yanfeng Wang. Audio-visual segmentation via unlabeled frame exploitation. In *Proceedings of the IEEE Conference on Computer Vision and Pattern Recognition*, 2024. 2
- [47] Jinxiang Liu, Yu Wang, Chen Ju, Chaofan Ma, Ya Zhang, and Weidi Xie. Annotation-free audio-visual segmentation. In *Proceedings of the IEEE/CVF Winter Conference on Applications of Computer Vision*, 2024. 2
- [48] Yuan Liu, Haodong Duan, Yuanhan Zhang, Bo Li, Songyang Zhang, Wangbo Zhao, Yike Yuan, Jiaqi Wang, Conghui He, Ziwei Liu, et al. Mmbench: Is your multi-modal model an all-around player? In *European Conference on Computer Vision*, pages 216–233. Springer, 2025. 5
- [49] Ilya Loshchilov and Frank Hutter. Sgdr: Stochastic gradient descent with warm restarts. *arXiv preprint arXiv:1608.03983*, 2016. 5
- [50] Ilya Loshchilov and Frank Hutter. Decoupled weight decay regularization. *arXiv preprint arXiv:1711.05101*, 2017. 5
- [51] Pan Lu, Swaroop Mishra, Tony Xia, Liang Qiu, Kai-Wei Chang, Song-Chun Zhu, Oyvind Tafjord, Peter Clark, and Ashwin Kalyan. Learn to explain: Multimodal reasoning via thought chains for science question answering. In *The 36th Conference on Neural Information Processing Systems (NeurIPS)*, 2022. 5

- [52] Chaofan Ma, Yuhuan Yang, Chen Ju, Fei Zhang, Jinxiang Liu, Yu Wang, Ya Zhang, and Yanfeng Wang. Diffusionseg: Adapting diffusion towards unsupervised object discovery. *arXiv preprint arXiv:2303.09813*, 2023. 2
- [53] Chaofan Ma, Yuhuan Yang, Chen Ju, Fei Zhang, Ya Zhang, and Yanfeng Wang. Open-vocabulary semantic segmentation via attribute decomposition-aggregation. *arXiv preprint arXiv:2309.00096*, 2023. 2
- [54] Chaofan Ma, Yuhuan Yang, Chen Ju, Fei Zhang, Ya Zhang, and Yanfeng Wang. Attrseg: open-vocabulary semantic segmentation via attribute decomposition-aggregation. *Advances in Neural Information Processing Systems*, 2024. 2
- [55] Chaofan Ma, Yuhuan Yang, Chen Ju, Yue Shi, Ya Zhang, and Yanfeng Wang. Freeseqdiff: Annotation-free saliency segmentation with diffusion models. In *IEEE International Conference on Acoustics, Speech and Signal Processing*. IEEE, 2025. 2
- [56] Adyasha Maharana, Prateek Yadav, and Mohit Bansal. D2 pruning: Message passing for balancing diversity and difficulty in data pruning. *arXiv preprint arXiv:2310.07931*, 2023. 3, 5, 6
- [57] Matthias Minderer, Alexey Gritsenko, Austin Stone, Maxim Neumann, Dirk Weissenborn, Alexey Dosovitskiy, Aravindh Mahendran, Anurag Arnab, Mostafa Dehghani, Zhuoran Shen, et al. Simple open-vocabulary object detection. In *European Conference on Computer Vision*, pages 728–755. Springer, 2022. 2
- [58] Anand Mishra, Shashank Shekhar, Ajeet Kumar Singh, and Anirban Chakraborty. Ocr-vqa: Visual question answering by reading text in images. In *ICDAR*, 2019. 5
- [59] OpenAI. Gpt-4v: Vision-language model, 2024. 1, 2
- [60] Adam Paszke, Sam Gross, Francisco Massa, Adam Lerer, James Bradbury, Gregory Chanan, Trevor Killeen, Zeming Lin, Natalia Gimelshein, Luca Antiga, et al. Pytorch: An imperative style, high-performance deep learning library. *Advances in neural information processing systems*, 32, 2019. 5
- [61] Mansheej Paul, Surya Ganguli, and Gintare Karolina Dzugaitė. Deep learning on a data diet: Finding important examples early in training. *Advances in neural information processing systems*, 34:20596–20607, 2021. 1, 2
- [62] Alec Radford et al. Learning transferable visual models from natural language supervision. In *International Conference on Machine Learning*, pages 8748–8763. PMLR, 2021. 1, 2, 3, 4, 5, 7
- [63] Christoph Schuhmann, Romain Beaumont, Richard Vencu, Cade W Gordon, Ross Wightman, Mehdi Cherti, Theo Coombes, Aarush Katta, Clayton Mullis, Mitchell Wortsman, Patrick Schramowski, Srivatsa R Kundurthy, Katherine Crowson, Ludwig Schmidt, Robert Kaczmarczyk, and Jenia Jitsev. LAION-5b: An open large-scale dataset for training next generation image-text models. In *Thirty-sixth Conference on Neural Information Processing Systems Datasets and Benchmarks Track*, 2022. 2, 5
- [64] Dustin Schwenk, Apoorv Khandelwal, Christopher Clark, Kenneth Marino, and Roozbeh Mottaghi. A-okvqa: A benchmark for visual question answering using world knowledge. In *European conference on computer vision*, pages 146–162. Springer, 2022. 5
- [65] Piyush Sharma, Nan Ding, Sebastian Goodman, and Radu Soricut. Conceptual captions: A cleaned, hypernymed, image alt-text dataset for automatic image captioning. In *Proceedings of ACL*, 2018. 5
- [66] Amanpreet Singh, Vivek Natarjan, Meet Shah, Yu Jiang, Xinlei Chen, Devi Parikh, and Marcus Rohrbach. Towards vqa models that can read. In *Proceedings of the IEEE Conference on Computer Vision and Pattern Recognition*, pages 8317–8326, 2019. 5
- [67] Ben Sorscher, Robert Geirhos, Shashank Shekhar, Surya Ganguli, and Ari Morcos. Beyond neural scaling laws: beating power law scaling via data pruning. *Advances in Neural Information Processing Systems*, 35:19523–19536, 2022. 1, 2
- [68] Bart Thomee, David A Shamma, Gerald Friedland, Benjamin Elizalde, Karl Ni, Douglas Poland, Damian Borth, and Li-Jia Li. Yfcc100m: The new data in multimedia research. *Communications of the ACM*, 59(2):64–73, 2016. 5
- [69] Keyu Tian, Yi Jiang, Zehuan Yuan, Bingyue Peng, and Liwei Wang. Visual autoregressive modeling: Scalable image generation via next-scale prediction. *Advances in neural information processing systems*, 37:84839–84865, 2025. 1
- [70] Kushal Tirumala, Daniel Simig, Armen Aghajanyan, and Ari Morcos. D4: Improving llm pretraining via document de-duplication and diversification. *Advances in Neural Information Processing Systems*, 36, 2024. 1, 2, 5, 6
- [71] Mariya Toneva, Alessandro Sordoni, Remi Tachet des Combes, Adam Trischler, Yoshua Bengio, and Geoffrey J Gordon. An empirical study of example forgetting during deep neural network learning. *arXiv preprint arXiv:1812.05159*, 2018. 1
- [72] Hugo Touvron, Thibaut Lavril, Gautier Izacard, Xavier Martinet, Marie-Anne Lachaux, Timothée Lacroix, Baptiste Rozière, Naman Goyal, Eric Hambro, Faisal Azhar, et al. Llama: Open and efficient foundation language models. *arXiv preprint arXiv:2302.13971*, 2023. 2, 4
- [73] Alex Jinpeng Wang, Kevin Qinghong Lin, David Junhao Zhang, Stan Weixian Lei, and Mike Zheng Shou. Too large; data reduction for vision-language pre-training. In *Proceedings of the IEEE/CVF International Conference on Computer Vision*, pages 3147–3157, 2023. 1, 2, 3, 5, 6
- [74] Haicheng Wang, Chen Ju, Weixiong Lin, Shuai Xiao, Mengting Chen, Yixuan Huang, Chang Liu, Mingshuai Yao, Jinsong Lan, Ying Chen, et al. Advancing myopia to holism: Fully contrastive language-image pre-training. *arXiv preprint arXiv:2412.00440*, 2024. 1
- [75] Haicheng Wang, Chen Ju, Weixiong Lin, Chaofan Ma, Shuai Xiao, Ya Zhang, and Yanfeng Wang. Contrast-unity for partially-supervised temporal sentence grounding. In *IEEE International Conference on Acoustics, Speech and Signal Processing*. IEEE, 2025. 2
- [76] Haicheng Wang, Zhemeng Yu, Gabriele Spadaro, Chen Ju, Victor Quéto, and Enzo Tartaglione. Folder: Accelerating multi-modal large language models with enhanced performance. *arXiv preprint arXiv:2501.02430*, 2025. 2

- [77] Yuhuan Yang, Chaofan Ma, Chen Ju, Ya Zhang, and Yanfeng Wang. Multi-modal prototypes for open-set semantic segmentation. *arXiv preprint arXiv:2307.02003*, 2023. 2
- [78] Yuhuan Yang, Chaofan Ma, Chen Ju, Fei Zhang, Jiangchao Yao, Ya Zhang, and Yanfeng Wang. Multi-modal prototypes for open-world semantic segmentation. *International Journal of Computer Vision*, 2024. 2
- [79] Lewei Yao, Runhui Huang, Lu Hou, Guansong Lu, Minzhe Niu, Hang Xu, Xiaodan Liang, Zhenguo Li, Xin Jiang, and Chunjing Xu. Filip: Fine-grained interactive language-image pre-training. In *Proceedings of the International Conference on Learning Representations*, 2022. 2, 7
- [80] Peter Young, Alice Lai, Micah Hodosh, and Julia Hockenmaier. From image descriptions to visual denotations: New similarity metrics for semantic inference over event descriptions. *Transactions of the Association for Computational Linguistics*, 2014. 5
- [81] Jiahui Yu, Zirui Wang, Vijay Vasudevan, Legg Yeung, Mojtaba Seyedhosseini, and Yonghui Wu. Coca: Contrastive captioners are image-text foundation models. *arXiv preprint arXiv:2205.01917*, 2022. 3, 7
- [82] Weihao Yu, Zhengyuan Yang, Linjie Li, Jianfeng Wang, Kevin Lin, Zicheng Liu, Xinchao Wang, and Lijuan Wang. Mm-vet: Evaluating large multimodal models for integrated capabilities. In *International conference on machine learning*. PMLR, 2024. 5
- [83] Lu Yuan, Dongdong Chen, Yi-Ling Chen, Noel Codella, Xiyang Dai, Jianfeng Gao, Houdong Hu, Xuedong Huang, Boxin Li, Chunyuan Li, et al. Florence: A new foundation model for computer vision. *arXiv preprint arXiv:2111.11432*, 2021. 2
- [84] Xiaohua Zhai, Basil Mustafa, Alexander Kolesnikov, and Lucas Beyer. Sigmoid loss for language image pre-training. In *Proceedings of the IEEE/CVF international conference on computer vision*, pages 11975–11986, 2023. 3, 7
- [85] Beichen Zhang, Pan Zhang, Xiaoyi Dong, Yuhang Zang, and Jiaqi Wang. Long-clip: Unlocking the long-text capability of clip. In *Proceedings of the European Conference on Computer Vision*. Springer, 2025. 3
- [86] Jingyi Zhang, Jiaying Huang, Sheng Jin, and Shijian Lu. Vision-language models for vision tasks: A survey. *IEEE Transactions on Pattern Analysis and Machine Intelligence*, 2024. 1
- [87] Xiaoman Zhang, Chaoyi Wu, Ziheng Zhao, Weixiong Lin, Ya Zhang, Yanfeng Wang, and Weidi Xie. Pmc-vqa: Visual instruction tuning for medical visual question answering. *arXiv preprint arXiv:2305.10415*, 2023. 1
- [88] Peisen Zhao, Lingxi Xie, Chen Ju, Ya Zhang, Yanfeng Wang, and Qi Tian. Bottom-up temporal action localization with mutual regularization. In *Proceedings of the European Conference on Computer Vision*. Springer, 2020. 2
- [89] Huangjie Zheng, Xu Chen, Jiangchao Yao, Hongxia Yang, Chunyuan Li, Ya Zhang, Hao Zhang, Ivor Tsang, Jingren Zhou, and Mingyuan Zhou. Contrastive attraction and contrastive repulsion for representation learning. *arXiv preprint arXiv:2105.03746*, 2021. 2
- [90] Deyao Zhu, Jun Chen, Xiaoqian Shen, Xiang Li, and Mohamed Elhoseiny. Minigpt-4: Enhancing vision-language understanding with advanced large language models. *arXiv preprint arXiv:2304.10592*, 2023. 2

# → : Squeeze Out Tokens from Sample for Finer-Grained Data Governance

## Supplementary Material

### A. Detailed Implementation and Results

**Pretraining Hyperparameters.** The standard configuration for our pre-training process is shown bellow. By default, we employ float32 as the numerical precision.

Config	Value
optimizer	AdamW
base learning rate	5e-5
weight decay	0.05
optimizer momentum	$\beta_1, \beta_2=0.9, 0.999$
batch size	1024
learning rate schedule	cosine decay
warmup epochs	5

**Model Architecture.** We detail the CLIP architecture from S to L as follows.

Model	Learning rate	Embedding dimension	Input resolution	Vision Transformer			Text Transformer		
				layers	width	heads	layers	width	heads
ViT-S/16	$5 \times 10^{-4}$	384	224	12	384	6	12	384	6
ViT-B/16	$5 \times 10^{-4}$	512	224	12	768	12	12	512	8
ViT-L/16	$5 \times 10^{-4}$	768	224	24	1024	16	12	768	12

### B. More Visualization

We show the modified samples from DataJuicer in Figure 7. To demonstrate the caption enhancement for various samples, we group the samples into rows according to the class confidence within images. Specifically, we categorized samples based on the top confidence scores of class predictions: scores below 30 were denoted as **low**, scores between 30 and 60 as **mid**, and scores above 60 as **high**. The confidence scores reflect the model’s certainty in identifying objects within the image.

High confidence scores underscore the reliability of identified objects in images. We define trustworthy samples as those whose top-confidence objects lie in **mid** to **high** confidence ranges. With more trustworthy classes, the increasing visual evidence coalesces into a cohesive representation of scene semantics. Take the subfigure(third row, second column) as an example; the class prediction 'hay' provides objects instead of a comprehensive view. Combined with 'harvester', we get an explicit scene of tractors and thrashers harvesting hay. Hence, multiple high-confidence classes make the scene content more specific, enabling the data governor to refine existing captions more confidently. Mutually verifying visual evidence and their synergistic interactions amplify the utilization of the LLMs’s inherent world knowledge, optimizing caption quality. Rather than modifying sentence structures (e.g., appending), LLMs seamlessly integrate visual evidence into the text descriptions.

When the highest-scoring objects within a sample exhibit **low** confidence scores, we prioritize the most salient objects as the primary visual evidence. And when the texts are non-descriptive, neglecting the primary objects, the visual and textual semantics are likely complementary. DataJuicer’s text branch  $\Psi_{\text{txt}}$  typically leverages high-confidence class information to refine captions, such as transforming generic terms (e.g., "car") into more specific descriptors (e.g., "racing car").

To conclude, DataJuicer enhances captions with detailed visual evidence from the vision branch and scene comprehension from the text branch.

### C. Limitation

Despite the gains brought by finer-grained data governance, there exist some limitations about DataJuicer. Our token view requires the model to embed data as tokens, e.g. image patches, and caption words. Though compatible with mainstream model architectures nowadays, there are possibilities that it would not benefit novel architectures proposed in the future.

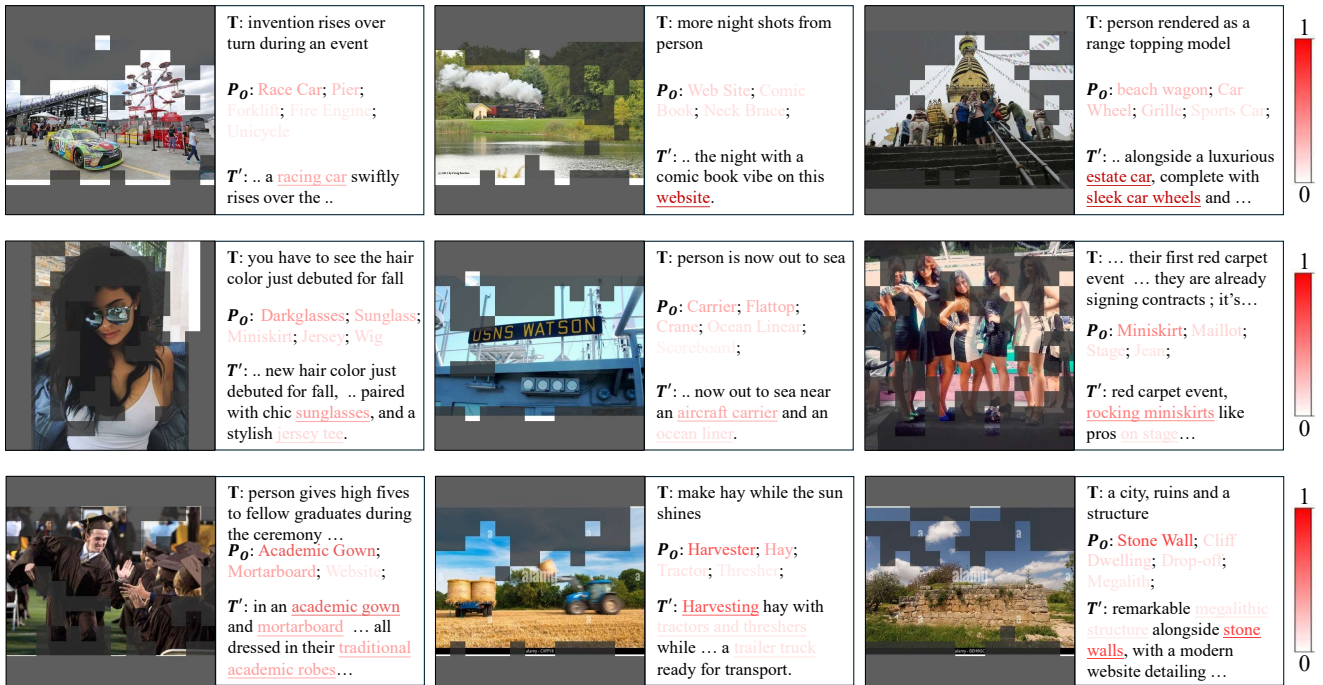


Figure 7. **More Visualizations.** Image patch elimination reduces the redundant pixels. As for text enhancement, DataJuicer completes the description with detailed class descriptions provided by the vision branch. The text branch infers the interactions among objects with world knowledge in LLM.